

## Evidence for Complex Superconducting Order Parameter Symmetry in the Low-Temperature Phase of $\text{UPt}_3$ from Josephson Interferometry

J. D. Strand\* and D. J. Van Harlingen†

Department of Physics and Frederick Seitz Materials Research Laboratory, University of Illinois at Urbana-Champaign, Urbana, Illinois 61801, USA

J. B. Kycia‡ and W. P. Halperin§

Department of Physics and Astronomy, Northwestern University, Evanston, Illinois 60208, USA

(Received 30 June 2009; published 4 November 2009)

We present data on the modulation of the critical current with applied magnetic field in  $\text{UPt}_3$ -Cu-Pb Josephson junctions and SQUIDs. The junctions were fabricated on polished surfaces of  $\text{UPt}_3$  single crystals. The shape of the resulting diffraction patterns provides phase-sensitive information on the superconducting order parameter. Our corner junction data show asymmetric patterns with respect to magnetic field, indicating a complex order parameter, and both our junction and SQUID measurements point to a phase shift of  $\pi$ , supporting the  $E_{2u}$  representation of the order parameter.

DOI: 10.1103/PhysRevLett.103.197002

PACS numbers: 74.70.Tx, 74.20.Rp, 74.50.+r

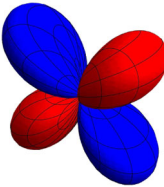
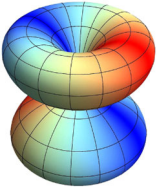
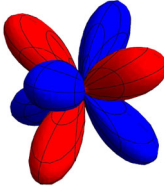
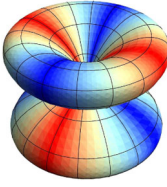
**Introduction.**—More than two decades after its discovery [1], the mechanism of superconductivity in the heavy-fermion superconductor  $\text{UPt}_3$  is still unknown. Although  $\text{UPt}_3$  was one of the first superconductors suspected to be unconventional due to its many unusual properties, the pairing symmetry has not been unambiguously determined. Perhaps most unusual is that it exhibits a double peak in the specific heat [2], indicating two distinct superconducting phases, with an initial transition at  $T_{c+} \approx 550$  mK and a second transition  $T_{c-} \approx 500$  mK. In addition to the high-temperature *A* phase and low-temperature *B* phase, subsequent measurements revealed a third phase at high magnetic fields [3]. Transport measurements show power law dependencies at low temperatures, revealing the presence of nodes in the superconducting gap [4,5]. Muon spin resonance showed signs of spontaneous magnetization, and thus time-reversal symmetry breaking (TRSB) in the low-temperature phase [6], but this result has not been reproduced in later measurements [7]. NMR studies of the Knight shift support a triplet pairing mechanism or possibly a singlet state with strong spin-orbit scattering [8]. There is also evidence that a very weak antiferromagnetic (AFM) moment in the basal plane coexists with superconductivity [9].

Numerous models for the pairing symmetry have been put forward to explain this complicated behavior, but the two best candidates are the singlet-state  $E_{1g}$  and triplet-state  $E_{2u}$  representations of the order parameter [10,11]. Both models feature a real order parameter in the *A* phase and a complex order parameter below the second transition in the *B* phase. Various efforts have been made to distinguish between these two theories on the basis of experiment [12–15], in particular, relying on details of transport properties, but the relatively subtle differences in node structure and gap magnitude have proven difficult to re-

solve. Perhaps the clearest difference between these models is the periodicity of phase winding in the order parameter, as seen in Table I. A rotation of  $90^\circ$  about the *c* axis causes a phase shift of  $\pi/2$  in the  $E_{1g}$  model, but a phase shift of  $\pi$  in the  $E_{2u}$  model. In this Letter, we propose to detect this difference in phase with Josephson interferometry, demonstrating the complex symmetry of the order parameter and helping to distinguish between these two models.

Josephson interferometry, used successfully to characterize the cuprates as *d* wave and  $\text{Sr}_2\text{RuO}_4$  as complex *p* wave [16–18], remains the most definitive phase-sensitive

TABLE I. Graphical depictions of the  $E_{1g}$  and  $E_{2u}$  models of the order parameter for  $\text{UPt}_3$ . Columns denote the high- and low-temperature (*A* and *B*, respectively) superconducting phases, and rows denote the two theoretical models.

	<i>A</i> Phase	<i>B</i> Phase
$E_{1g}$		
	$\Delta(k) = \Delta(T)k_x k_z$	$\Delta(k) = \Delta(T)(k_x + ik_y)k_z$
$E_{2u}$		
	$\bar{d}(k) = \Delta(T)(k_x^2 - k_y^2)k_z \hat{z}$	$\bar{d}(k) = \Delta(T)(k_x + ik_y)^2 k_z \hat{z}$

test of the order parameter of unconventional superconductors. In this technique, a superconducting weak link is created between two superconductors—in our case, a single crystal of  $\text{UPT}_3$  and a film of the conventional superconductor Pb. Applying a magnetic field to this junction perpendicular to the current flow creates a phase gradient along the junction that alters the local supercurrent density. Any intrinsic phase differences arising from the order parameter symmetry will also affect the current density. In the short junction limit in which fields from the tunneling current (and the small AFM moment) can be neglected, the critical current ( $I_c$ ) can be given as a function of external flux ( $\Phi_{\text{ext}}$ ) and intrinsic phase difference ( $\delta$ ) by the following:

$$I_c(\Phi_{\text{ext}}) = I_0 \left| \frac{\sin(\pi\Phi_{\text{ext}}/\Phi_0 + \delta/2)}{\pi\Phi_{\text{ext}}/\Phi_0} \right|. \quad (1)$$

In the case of uniform  $s$  wave superconductors, this results in the conventional Fraunhofer diffraction pattern shape for plots of critical current vs applied magnetic field. Even in a superconductor with an anisotropic order parameter, as long as the junction is on a single flat crystal face, the pattern will look Fraunhofer. This is because tunneling probability falls off exponentially with barrier thickness and so the Josephson current effectively probes a single  $k$ -space direction. If, however, the junction wraps around the corner of a superconductor with a sign change in the order parameter between the two tunneling directions, part of the junction will probe each direction, and the phase shift will cause a distinctive change in the diffraction pattern. The predicted patterns for corner junctions in the low-temperature phase are given in Fig. 1. All the measurements in this Letter were taken well inside the  $B$  phase of  $\text{UPT}_3$ , where we can test for complex superconducting order. Measurements of the  $A$  phase as well as the cross-over between phases will be the topic of future work.

*Experiment.*—The  $\text{UPT}_3$  crystals were grown in an electron-beam floating zone furnace, and have a measured residual resistivity ratio (RRR) of greater than 900, in some cases as high as 1100, indicating their exceptional purity. We polished the surfaces with  $0.3 \mu\text{m}$  diamond lapping films and then glued them to a glass substrate with Pyralin® polyimide coating. After masking with a dry photoresist, the surfaces were ion milled and 150 nm of Cu was evaporated as a normal metal barrier, followed by 800 nm of Pb as the superconducting counter-electrode. Junction dimensions were typically  $50 \times 100 \mu\text{m}$ , with an effective thickness of  $\approx 1 \mu\text{m}$ , after including the superconducting penetration depths. Previous experiments on  $\text{UPT}_3$  have had to take great care to avoid magnetic flux trapping [19], so the samples were cooled in a Kelvinox® dilution refrigerator with Cryoperm® and lead cans to provide the necessary magnetic shielding ( $H_{\text{residual}} \approx 10^{-4}$  G). The junction voltages were in the picovolt range, and so were measured with a superconducting quantum

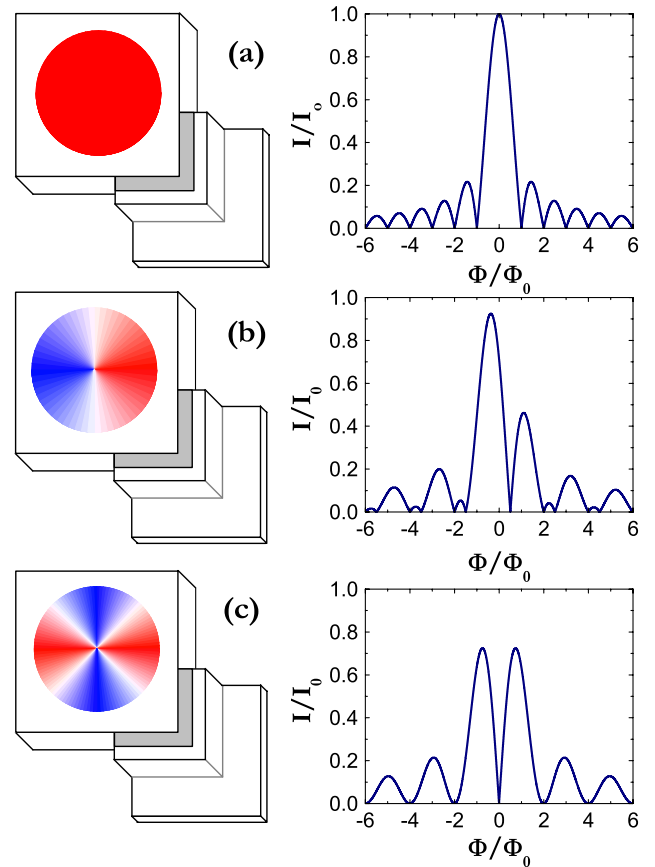


FIG. 1 (color online). Planar representations of the order parameter laid on top of a schematic of a corner junction, with the corresponding diffraction pattern placed alongside. (a) An  $s$ -wave order parameter produces the classic Fraunhofer pattern. (b) The  $E_{1g}$   $B$  phase produces an asymmetric double peak. (c) The  $E_{2u}$   $B$  phase produces a symmetric double peak.

interference device (SQUID) potentiometer circuit, in which an inductively coupled SQUID detected the current flowing through a known resistor in parallel with the junction.

The junctions exhibited nearly ideal resistively shunted junction (RSJ) behavior, as well as showing Shapiro steps when an ac modulation was applied. We measured 11 junctions fabricated on a single crystal face, which displayed diffraction patterns that were nearly Fraunhofer and symmetric around zero field, indicating uniform phase and no trapped vortices. Examples of these measurements, as well as a sample photo, can be seen in Fig. 2. It is worth mentioning that even though the  $B$  phase of  $\text{UPT}_3$  is expected to be chiral and exhibit TRSB, similar to  $\text{Sr}_2\text{RuO}_4$ , we saw none of the evidence for chiral domains in  $\text{UPT}_3$  that were seen in  $\text{Sr}_2\text{RuO}_4$  [18], such as hysteresis or switching noise.

We also measured three junctions fabricated so that they straddled the corner between the  $a$  and  $b$  axes. These corner junctions behaved quite differently than the edge junctions. In all cases, the diffraction patterns they pro-

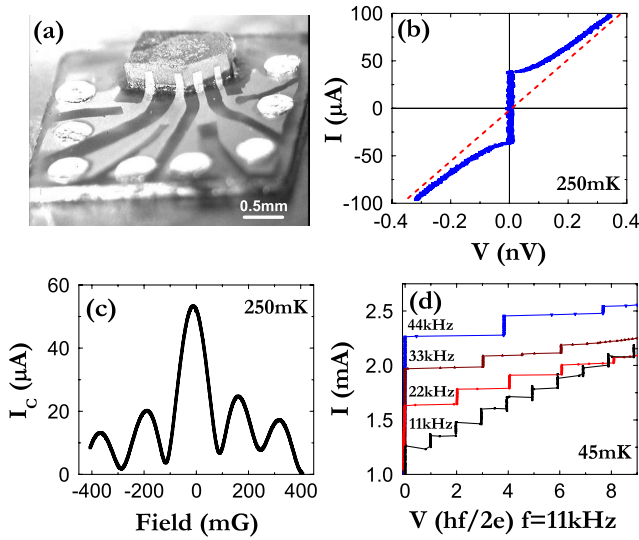


FIG. 2 (color online). (a) A photograph of one of our samples—the crystal is the large block in the upper middle with four edge junctions evaporated on its surface. The lines of Pb film and indium pads are also visible. (b) A characteristic IV plot for a junction, showing classic RSJ behavior. (c) A diffraction pattern for one of our edge junctions, exhibiting a nearly Fraunhofer shape. (d) Shapiro steps from a junction, confirming Josephson behavior.

duced exhibited features that were asymmetric with respect to field polarity. The asymmetry was not caused by the self-field effect of the current through the junction because the pattern was symmetric with respect to the direction of current flow. Changing temperatures affected the magnitude of the critical current, as expected, but left the shape of the patterns unchanged. This asymmetry with respect to field polarity is a characteristic sign of a complex order parameter symmetry and TRSB.

Aside from the ever-present asymmetry, the corner junction patterns varied between thermal cycles of the same junction, with three or four qualitatively similar patterns recurring. These changes require a dynamic mechanism to explain. The most obvious candidate is vortex trapping near the junctions. We can consistently get vortex-free edge junctions, indicating that our magnetic shielding and slow cooling cycles are sufficient to prevent flux-trapping in the bulk of the junctions. The corners of our samples, however, could provide a pinning location as surface damage can easily suppress superconductivity in an unconventional superconductor. Even well-polished surfaces are prone to chipping at the edge, and faceting at the region where two surfaces meet is probable.

With this in mind, we have tried modeling corner junctions combining an intrinsic phase shift with a vortex trapped at the corner. We tested phase shifts corresponding to the three candidate symmetries: 0 (*s*-wave),  $\pi/2$  ( $E_{1g}$ ), and  $\pi$  ( $E_{2u}$ ). We modeled a vortex as a Gaussian contribu-

tion to the flux through the junction with integrated flux =  $\Phi_0/2$  and width equal to 3% of the junction width. The junctions are not perfectly symmetric around the corner, and so we allowed the location of the corner (and thus the vortex) to vary by 10% of the junction width. We then compared the resulting patterns with our data. We do not claim to have modeled the junctions exactly, but focused on matching the number and relative size of the central peaks in the diffraction patterns. In a series of cooldowns, patterns like that in Fig. 3(a) occurred the majority of the time, suggesting that it is the vortex-free state. It also matches well with a phase shift of  $\pi$  with no vortex. Though qualitative, we found this comparison supported the  $E_{2u}$  representation more strongly than the  $E_{1g}$  representation. Comparisons of representative diffraction patterns to simulations are given in Fig. 3.

In an effort to avoid the complications caused by the material properties of the corners, we fabricated two junctions, one on either side of the corner, forming a dc SQUID with a loop area of  $300 \mu\text{m}^2$ , which is much larger than the magnetic area of the individual junctions ( $\approx 25 \mu\text{m}^2$ ). In this case, an intrinsic phase difference in the crystal will show up as a shift in the peak of the critical current modulation, as given by

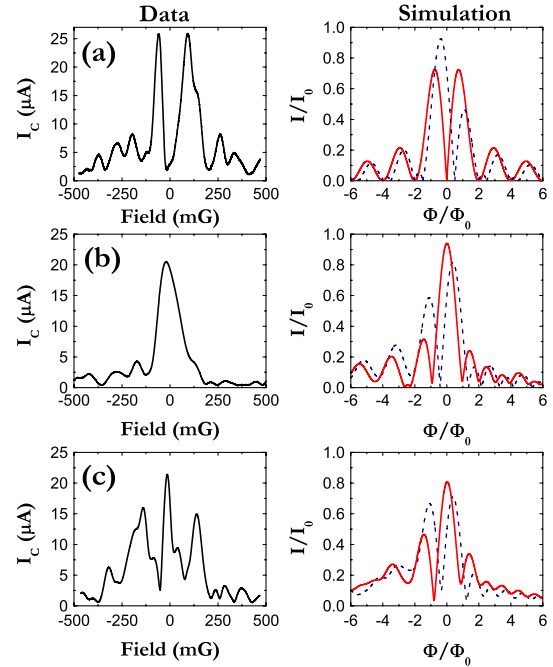


FIG. 3 (color online). Comparisons of corner junction diffraction patterns ( $T = 60 \text{ mK}$ ) with simulations. The three data plots are representative of the three recurring patterns we observed. The simulations assume a single vortex located at the corner of the junction, with the location of the corner allowed to vary by 10% of junction width. Simulations with solid lines assume the  $E_{2u}$  representation, and simulations with dashed lines assume the  $E_{1g}$  representation.

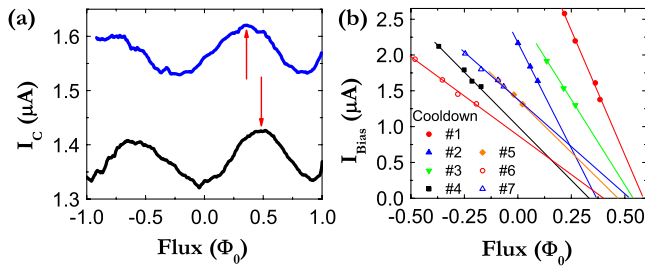


FIG. 4 (color online). (a) Two SQUID modulation curves taken at 90 mK with different bias currents—arrows denote the peaks and highlight the shift in position caused by asymmetric current flow. The arrow locations for these and other curves correspond to data points in plot (b). (b) Extrapolations to zero bias current for seven thermal cycles of the corner SQUID. The lines cluster around a phase shift of  $0.5\Phi_0$ .

$$I_c(\Phi_{\text{ext}}) = 2I_0 \left| \cos\left(\pi \frac{\Phi_{\text{ext}}}{\Phi_0} + \frac{\delta}{2}\right) \right|. \quad (2)$$

Unlike a single junction, the periodic modulation of a SQUID does not provide a central peak to reveal the zero point of magnetic flux, so extra care is required to rule out extrinsic shifts in the pattern. If the two junctions are not identical, unequal current flow between the branches of the loop will couple field into the SQUID, shifting the pattern. To account for this, we bias the SQUID at various current levels as shown in Fig. 4(a), noting peak location at each current, and then extrapolate the peak location to zero bias current [20]. In order to account for residual external field or trapped flux, we performed several thermal cycles, with the results plotted in Fig. 4(b). The results cluster around  $\Phi_0/2$ , corresponding to a phase shift of  $\pi$ , which agrees with our corner junction results and also supports the  $E_{2u}$  model.

**Conclusions.**—In summary, we have fabricated Josephson junctions on high-quality single crystals of  $\text{UPT}_3$  and used them to perform phase-sensitive measurements of the superconducting order parameter. There is strong evidence for a complex component of the order parameter from the asymmetry with respect to field polarity in the diffraction patterns, but we found no sign of chiral domains in our edge junctions. By comparing our corner junction results with simulations involving vortex trapping at the corner and from shifts in SQUID modulation curves, we find evidence for an intrinsic phase shift of  $\pi$  for a  $90^\circ$  rotation, in agreement with the  $E_{2u}$  representation of the order parameter. We are continuing further measurements with different surface treatments, including as-grown crystal faces, in order to reduce the effect of vortices, as well as studying the crossover between the  $A$  and  $B$  phases.

The measurements were carried out at the University of Illinois in the Frederick Seitz Materials Research Laboratory and supported by NSF Grant No. DMR07-

05214. The  $\text{UPT}_3$  crystals were grown and annealed at Northwestern University supported by the DOE Basic Energy Sciences Grant No. DE-FG02-05ER46248. We acknowledge the help of J. Davis, J. Pollanen, H. Choi, T. Lippman, and W. Gannon with crystal growth and characterization.

\*strand2@illinois.edu

†dvh@illinois.edu

‡jkycia@scimail.uwaterloo.ca

§w-halperin@northwestern.edu

- [1] G. R. Stewart, Z. Fisk, J. O. Willis, and J. L. Smith, Phys. Rev. Lett. **52**, 679 (1984).
- [2] R. A. Fisher, S. Kim, B. F. Woodfield, N. E. Phillips, L. Taillefer, K. Hasselbach, J. Flouquet, A. L. Giorgi, and J. L. Smith, Phys. Rev. Lett. **62**, 1411 (1989).
- [3] S. Adenwalla, S. W. Lin, Q. Z. Ran, Z. Zhao, J. B. Ketterson, J. A. Sauls, L. Taillefer, D. G. Hinks, M. Levy, and B. K. Sarma, Phys. Rev. Lett. **65**, 2298 (1990).
- [4] K. Behnia, L. Taillefer, J. Flouquet, D. Jaccard, K. Maki, and Z. Fisk, J. Low Temp. Phys. **84**, 261 (1991).
- [5] H. Suderow, J. P. Brison, A. Huxley, and J. Flouquet, J. Low Temp. Phys. **108**, 11 (1997).
- [6] G. M. Luke, A. Keren, L. P. Le, W. D. Wu, Y. J. Uemura, D. A. Bonn, L. Taillefer, and J. D. Garrett, Phys. Rev. Lett. **71**, 1466 (1993).
- [7] P. D. de Reotier, A. Huxley, A. Yaouanc, J. Flouquet, P. Bonville, P. Imbert, P. Pari, P. Gubbens, and A. Mulders, Phys. Lett. A **205**, 239 (1995).
- [8] H. Tou, Y. Kitaoka, K. Asayama, N. Kimura, Y. Onuki, E. Yamamoto, and K. Maezawa, Phys. Rev. Lett. **77**, 1374 (1996).
- [9] G. Aeppli, E. Bucher, C. Broholm, J. Kjernes, J. Baumann, and J. Hufnagl, Phys. Rev. Lett. **60**, 615 (1988).
- [10] K. A. Park and R. Joynt, Phys. Rev. B **53**, 12346 (1996).
- [11] J. A. Sauls, Adv. Phys. **43**, 113 (1994).
- [12] M. R. Norman and P. J. Hirschfeld, Phys. Rev. B **53**, 5706 (1996).
- [13] M. J. Graf, S. Yip, and J. A. Sauls, Phys. Rev. B **62**, 14393 (2000).
- [14] W. C. Wu and R. Joynt, Phys. Rev. B **65**, 104502 (2002).
- [15] R. Joynt and L. Taillefer, Rev. Mod. Phys. **74**, 235 (2002).
- [16] D. A. Wollman, D. J. Van Harlingen, J. Giapintzakis, and D. M. Ginsberg, Phys. Rev. Lett. **74**, 797 (1995).
- [17] K. D. Nelson, Z. Q. Mao, Y. Maeno, and Y. Liu, Science **306**, 1151 (2004).
- [18] F. Kidwingira, J. D. Strand, D. J. Van Harlingen, and Y. Maeno, Science **314**, 1267 (2006).
- [19] A. Sumiyama, R. Hata, Y. Oda, N. Kimura, E. Yamamoto, Y. Haga, and Y. Onuki, Phys. Rev. B **72**, 174507 (2005).
- [20] D. A. Wollman, D. J. Van Harlingen, W. C. Lee, D. M. Ginsberg, and A. J. Leggett, Phys. Rev. Lett. **71**, 2134 (1993).